IOP Publishing Superconductor Science and Technology
Supercond. Sci. Technol. 31 (2018) 074002 (9pp) https://doi.org/10.1088/1361-6668/aac11c

Development of high J_c Bi2223/Ag thick film materials prepared by heat treatment under low P_{O2}

Y Takeda[1], J Shimoyama[2], T Motoki[2], S Nakamura[3], T Nakashima[4], S Kobayashi[4] and T Kato[4]

[1] Department of Applied Chemistry, The University of Tokyo, 7-3-1 Hongo, Bunkyo-ku, Tokyo 113-8656, Japan
[2] Department of Physics and Mathematics, Aoyama Gakuin University, 5-10-1 Fuchinobe, Chuo-ku, Sagamihara, Kanagawa 252-5258, Japan
[3] TEP Co., Ltd., 2-20-4 Kosuge, Katsushika-ku, Tokyo 124-0001, Japan
[4] Sumitomo Electric Industries, Ltd., 1-1-3 Shimaya, Konohana-ku, Osaka 554-0024, Japan

E-mail: ytakeda@g.ecc.u-tokyo.ac.jp

Received 8 March 2018, revised 12 April 2018
Accepted for publication 30 April 2018
Published 18 May 2018

Abstract

In general, a dense and *c*-axis grain-oriented microstructure is desirable in order to achieve the high critical current properties of Bi2223 polycrystalline materials. On the other hand, our recent studies have shown that precise control of the chemical compositions of Bi2223 is also effective for the enhancement of intergrain J_c. In this study, the development of Bi2223 thick film materials with high critical current properties was attempted by controlling both the microstructure and the chemical compositions. A high intergrain J_c of $\sim$8 kA cm^{-2} at 77 K of a film with $\sim$40 μm^t was achieved by increasing the Pb substitution level for the Bi site and controlling the nonstoichiometric chemical compositions. Furthermore, it was revealed that an increase in the thickness enabled us to obtain high I_c films suitable for practical applications. In contrast, there are still issues, especially in controlling the grain alignment at the inner part of the film, which suggests that the J_c properties of thick film materials could be further improved by forming a more ideal microstructure, as realized in the Bi2223 filaments of multi-filamentary Ag-sheathed tapes.

Keywords: Bi2223, BSCCO, J_c, thick films

(Some figures may appear in colour only in the online journal)

1. Introduction

Bi2223 ($Bi_{2-x}Pb_xSr_2Ca_2Cu_3O_y$) is one of the most promising cuprate superconductors for practical applications. The Ag-sheathed Bi2223 commercial tapes, DI-BSCCO, show high critical current (I_c) characteristics of up to 200 A at 77 K in the self-field [1]. Therefore, they have been widely used for power cables [2] and superconducting magnets [3] in various applications, such as motors [3] and high-resolution NMR systems [4]. In addition, Bi2223 polycrystalline bulk materials are used as superconducting current leads with low thermal conductivity for superconducting magnet systems cooled by cryocoolers [5]. The critical current properties of these practical polycrystalline materials have been mainly improved by controlling their microstructure.

Since Bi2223 crystals usually have a thin plate-like shape with a wide *ab*-plane parallel to the superconducting CuO_2 plane, and the critical current density (J_c) in the *ab*-plane is much higher than that along the *c*-axis direction, the formation of a *c*-axis-oriented microstructure is crucially important in achieving high J_c properties in polycrystalline materials. Bi2223 crystals are known to easily cleave at the weakly coupled Bi–O double layer, and hence mechanical pressing and flat rolling enable us to fabricate *c*-axis-oriented Bi2223 polycrystalline materials [6]. The latter process is generally adopted in the production of practical tapes [3] and the former

 © 2018 IOP Publishing Ltd Printed in the UK

is applied for bulk materials [5] after the formation of the Bi2223 phase. These mechanical pressing and rolling processes are also effective in densifying the superconducting oxide core, which is another key to synthesizing high J_c polycrystalline materials. Furthermore, the controlled-over-pressure sintering method [7] under careful control of oxygen partial pressure (P_{O2}) is applied in the fabrication of DI-BSCCO tapes and the high J_c of $\sim 6 \times 10^4$ A cm^{-2} at 77 K is uniformly achieved in long tapes. Controlling the microstructure described above, i.e. *c*-axis grain orientation and densification of the superconducting oxide core, is indispensable in preparing polycrystalline materials with high J_c properties.

On the other hand, an improvement of the superconducting properties of layered cuprate superconductors can also be achieved by controlling the nonstoichiometric chemical compositions. In our previous studies, the critical temperature (T_c) of the Bi2223 practical tapes was found to be enhanced up to 115 K by the addition of a post-annealing process above 700 °C [8]. This process is thought to change the nonstoichiometric cation compositions close to the integral ratio, (Bi,Pb): Sr: Ca: Cu ~2: 2: 2: 3, resulting in an increase in the superconducting condensation energy. However, the precipitates of $(Pb,Bi)_3Sr_2Ca_2CuO_y$ (Pb3221) containing tetravalent lead ions easily generate during post annealing [9, 10], which leads to a deterioration of the coupling between Bi2223 crystals. It was revealed that the generation of Pb3221 was successfully suppressed by post annealing under moderately reducing atmospheres, $P_{O2} <$ 1 kPa [11]. Such careful control of the cation compositions leads to an enhancement of both T_c and intergrain J_c, $J_{c\ (intergrain)}$. Our recent study revealed that the $J_{c\ (intergrain)}$ of a Bi2223 sintered bulk was largely improved by reductive post annealing under $P_{O2} = 500$ Pa at 740 °C [12].

In addition, Pb doping for the Bi site in Bi-based superconductors is effective at increasing hole carriers [13] because lead ions and bismuth ions are divalent and trivalent, respectively, in the Bi-based superconductors, while oxygen content does not largely decrease. Moreover, previous studies showed that the electromagnetic anisotropy of Bi2212 $[(Bi,Pb)_2Sr_2CaCu_2O_y]$ single crystals dramatically decreased with an increase in the Pb substitution level [14, 15]. The $J_{c\ (intergrain)}$ of the polycrystalline materials of cuprate superconductors is generally considered to be enhanced by decreasing the anisotropy achieved through carrier overdoping and/or by an improvement in conductivity at the blocking layer through doping, such as Pb-doping for Bi-based superconductors [14, 15] and Re-doping for Hg-based superconductors [16]. However, the relationship between the critical current properties and the Pb-doping level of Bi2223 polycrystalline materials has not been empirically clarified yet. The final oxygen annealing process at low temperatures below 400 °C to increase the oxygen content of the Bi2223 phase is also effective for enhancing $J_{c\ (intergrain)}$. This indicates that further improvement of the $J_{c\ (intergrain)}$ of Bi2223 polycrystalline materials, such as bulks and thick films, could be expected by the formation of a dense and *c*-axis-oriented microstructure, as well as precise control of both cation and oxygen compositions, which has already been achieved in Bi2223 commercial tapes.

From this contextual background, the development of Bi2223 polycrystalline materials with high critical current properties was attempted through chemical approaches. We focused on thick film materials in the present study because controlling the microstructure, such as grain orientation and densification, is considered to be relatively easy. Furthermore, Bi2223 thick films with high critical current properties are thought to be promising materials for various applications, such as current leads and magnetic shields. Firstly, the constituent phases of the precursor films were systematically varied for the synthesis of dense and *c*-axis-aligned Bi2223 films. The effects of the premix level of Bi2223 crystals in the precursor films on the microstructure of sintered films were investigated. Premixed Bi2223 grains should be strongly *c*-axis oriented by uniaxial pressing before sintering. Secondly, physical properties, including the grain coupling, of the *c*-axis-aligned Bi2223 films with various Pb substitution levels were evaluated. Finally, the fabrication of thick films with high I_c was attempted by increasing the film thickness to derive the potential for current carrying applications. In this study, sintering was performed under a slightly lower P_{O2} of 3 kPa than the typical condition (~8 kPa), which is adopted for the fabrication of commercial tapes [7]. Our previous studies revealed that sintering under $P_{O2} < 5$ kPa is effective for both the fast phase formation of Bi2223 and the suppression of the grain growth of the secondary phases [17].

2. Experimental

2.1. Preparing slurries and green films

Thick film samples were fabricated from slurries containing oxide precursor powder and organic components. The nominal cation ratio of the precursor powder was controlled to be Bi: Pb: Sr: Ca: Cu ~2.05−*x*: *x*: 1.9: 2.0: 3.0 ($x = 0.35$–0.39) by mixing two kinds of powder. One powder is referred to as '2212' powder hereafter, which is the calcined powder of Bi2223 with $x = 0.35$ (the typical value in Bi2223 materials). This 2212 powder was obtained by heating oxides at 780 °C in air composed of Bi2212, Ca_2PbO_4 and other oxides. Another powder is referred to as '2223' powder, which was prepared by sintering the calcined powder above 800 °C under low $P_{O2} < 3$ kPa and pulverization. Bi2223 is the main phase of this powder. In the preparation of the slurries, these two kinds of powder were mixed into a nominal molar ratio of 2212: 2223 = X_{2212} : 1–X_{2212}, where X_{2212} represents the ratio of 2212 powder in the mixed powder. Organic solvents (EtOH/BuOH), a binder, other organic components and nylon-coated iron balls were added to the precursor powder in a bottle, and ball milling was performed for ~50 h to obtain homogeneous slurries with moderate viscosity. Then, the green thick films were fabricated by a simple doctor-blade casting method. The slurries were cast into green tapes with a thickness of 400 μm on an acrylic flat plate using a razor blade and vinyl tape banks. After drying in air, rectangular

green film samples of $\sim 5 \times 7\,\mathrm{mm}^2$ cut from the green tapes were placed on Ag foil substrates with a thickness of 50 μm.

2.2. Fabrication of thick film samples by heat treatment under low P_{O2}

After heating gradually up to 500 °C in air to remove the organic components, the green film samples were annealed at 600 °C for 12 h in flowing Ar to decrease the oxygen content of the Bi2212 and Bi2223 crystals in the tapes. Then, the oxide thick films were sandwiched by Ag foils to suppress the vaporization of Bi and Pb during sintering, and were uniaxially pressed under ~1 GPa to densify the oxide layer. It is considered that the *c*-axis orientation of the Bi2223 crystals is promoted by the uniaxial pressing for samples with $X_{2212} < 1$. Note that pre-annealing in flowing Ar at 600 °C is essential to prevent the Ag foils from swelling owing to the oxygen released from the Bi2212 and the Bi2223 crystals during heating. The first sintering to form the Bi2223 phase from mixed 2212 powder was performed at 810 °C for 6–18 h under $P_{O2} = 3$ kPa by flowing a mixed gas (3% O_2/Ar). After the first sintering, intermediate uniaxial pressing under ~1 GPa was conducted. Further densification and *c*-axis grain alignment in the oxide core could be achieved by this intermediate pressing. The second sintering to recover grain coupling deteriorated by the intermediate pressing was performed at 800–820 °C for 6 h under $P_{O2} = 3$ kPa. The typical film thickness of the samples after the second sintering was ~40 μm, and the film thickness was easily increased by stacking the green films. In each sintering, the samples were slowly cooled down to 20 °C below the sintering temperature for 3 h to crystalize the amorphous phase originating from the liquid phase in the reaction forming the Bi2223 phase. Some film samples were post-annealed at 760 °C for 48–100 h under $P_{O2} = 200$–500 Pa in order to control the nonstoichiometric cation compositions without the generation of Pb3221 precipitates. Oxygen annealing at 300 °C–350 °C for 6–12 h was carried out for some samples after the second sintering and all post-annealed samples in reducing atmospheres to increase the oxygen content of Bi2223 to achieve a carrier slightly overdoped state. Samples to evaluate the relationship between the *c*-axis length and the cation compositions were annealed in air at 600 °C and quenched to room temperature to reduce the difference in the oxygen content among the samples.

2.3. Characterization

Constituent phases and lattice constants were examined by surface x-ray diffraction (XRD) using a RIGAKU Ultima IV. The *c*-axis length of the Bi2223 phase was estimated from the 0024 peak, and Ag was used as an internal standard. Microstructures of the films were observed by field emission scanning electron microscopy (FE-SEM, Carl Zeiss AG-ULTRA 55) and a 400 kV transmission electron microscope (TEM, JEOL JEM-4010). The local chemical composition of the crystals in the films was analyzed by wavelength-dispersive spectroscopy (WDS) equipped with an electron probe micro-analyzer (EPMA, JEOL JXA-8200S). The superconducting properties were evaluated by magnetization measurements using a SQUID magnetometer (MPMS, Quantum Design). Resistivity and transport measurements were performed by the conventional four-point-probe method by applying ac or dc current, respectively, using a Physical Property Measurement System (Quantum Design). Ag foils covering the samples were removed as needed in these characterizations. The $J_{c\ (intergrain)}$ under a zero external field was examined by the remanent magnetization measurement. The irreversibility line was determined through measurements of the temperature dependence of resistivity under various fields using a criterion of $\rho = 10^{-7}\,\Omega\,\mathrm{cm}$. In all the above measurements, magnetic fields were always applied normal to the surface of the films, i.e. almost parallel to the *c*-axis of the Bi2223 crystals.

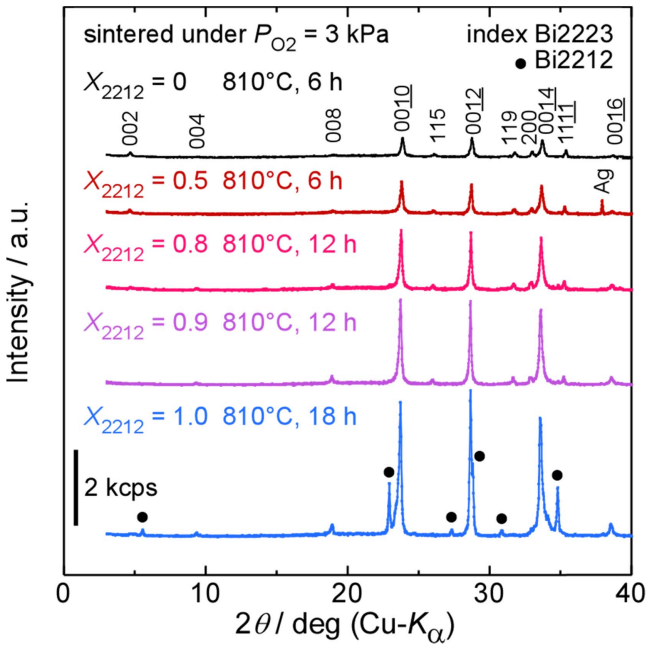

Figure 1. Surface x-ray diffraction patterns of the film samples after the first sintering with various X_{2212}.

3. Results and discussion

3.1. Effects of the constituent phases of the precursor on the microstructure and intergrain J_c of the films

2223 powder with a fixed Pb substitution level of $x = 0.35$ was obtained by sintering 2212 powder at 820 °C for 12 h under $P_{O2} = 3$ kPa and pulverization. In order to determine the optimal mixing ratio of Bi2212 and Bi2223 grains in the precursor, the thick film samples with ~40 μm^t and various X_{2212} were prepared by sintering at 800 °C–820 °C under $P_{O2} = 3$ kPa and evaluating their microstructures and $J_{c\ (intergrain)}$. Surface XRD patterns of the typical first-sintered samples are shown in figure 1. As can be clearly seen, Bi2223 was the main phase in the samples with $X_{2212} < 0.9$ after the first sintering for 6–12 h, while the unreacted Bi2212 crystals

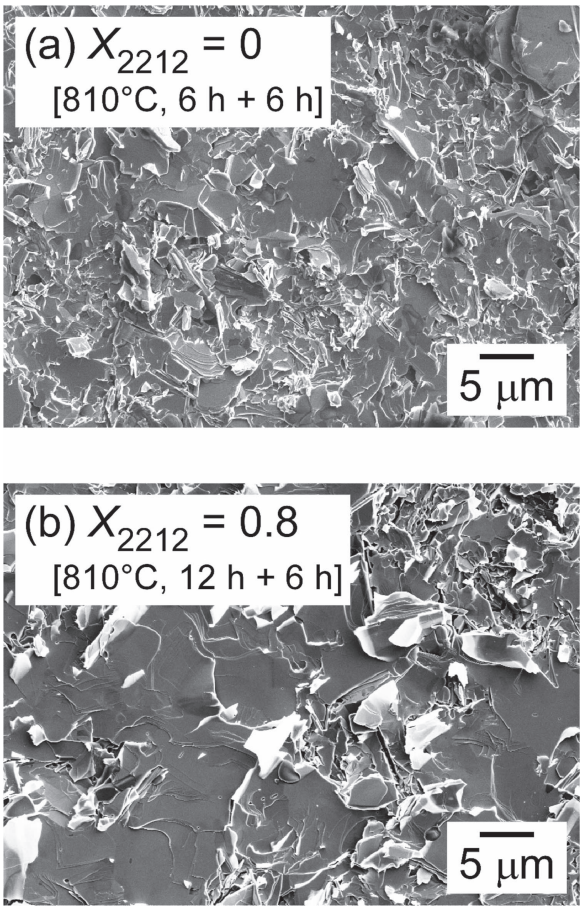

Figure 2. Surface secondary electron images of the film samples with (a) $X_{2212} = 0$ and (b) $X_{2212} = 0.8$ after the second sintering.

remained in the sample with $X_{2212} = 1.0$, though the longer first sintering for 18 h was applied. Bi2223 crystals in the precursor powder, which had been expected to contribute to the *c*-axis grain alignment, were found to promote the formation of the Bi2223 phase in the film samples. The relatively strong intensity of the 00*l* peaks of the Bi2223 phase in all samples means that a *c*-axis-oriented microstructure formed near the Ag surface. In addition, the intensity of the 00*l* peaks was stronger for the sample with larger X_{2212}, suggesting that a larger fraction of calcined powder composed of unreacted Bi2212 and other phases in the precursor films is preferable to obtain the strongly *c*-axis oriented microstructure. Most of these results were not expected before starting the present study. The *c*-axis orientation in the surface of the samples with larger X_{2212} (particularly $X_{2212} > 0.7$) was found to be further strengthened by intermediate pressing under ~1 GPa and then the second sintering for 6 h.

To evaluate the degree of the grain orientation, the surface microstructure of the film samples was observed by SEM. Figure 2 shows the secondary electron images taken for the surface of the samples with $X_{2212} = 0$ and 0.8 after the second sintering. In the surface XRD patterns, it was confirmed that both samples were composed almost entirely of a Bi2223 single phase, and the intensity of the 00*l* peaks of the Bi2223 phase of the sample with $X_{2212} = 0.8$ was approximately four times higher than that of the sample with

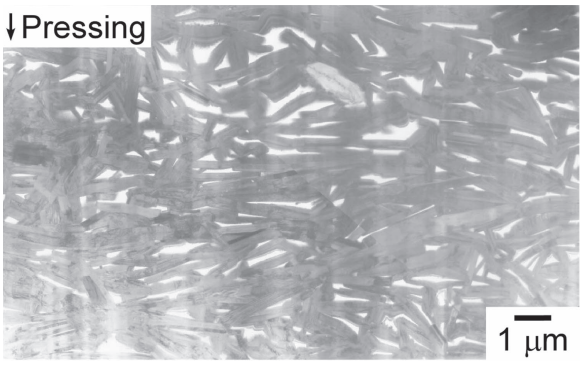

Figure 3. A cross-sectional TEM image of the inner part of the film sample with $X_{2212} = 0.8$ after the second sintering at 810 °C for 12 h + 6 h under $P_{O2} = 3$ kPa.

$X_{2212} = 0$. *c*-axis-aligned Bi2223 plate-like crystals were observed in both surfaces, while the grain size and the degree of the *c*-axis orientation were clearly different. The typical grain size of the sample with $X_{2212} = 0$ was ~5 μm, which is smaller than that of the sample with $X_{2212} = 0.8$, > 10 μm. The degree of the *c*-axis orientation, i.e. the ratio of the *c*-axis-oriented grains in the surface of the sample with $X_{2212} = 0.8$, was higher than that of the sample with $X_{2212} = 0$. These characteristics of the microstructures coincide well with the results of the surface XRD. Since the strongly *c*-axis-aligned Bi2223 grains are known to easily grow near the Ag interface [18] intermediating the liquid phase that arises with the formation reaction of the Bi2223 phase, the highly *c*-axis grain-oriented surface was thought to form in the films with larger X_{2212}.

On the other hand, it was also found that there was room for improvement in the microstructure of the inner part of the film. A cross-sectional TEM image of the inner region of the sample with $X_{2212} = 0.8$ after the second sintering is shown in figure 3. Many Bi2223 plate-like crystals aligned normal to the uniaxial pressing direction, that is, parallel to the film surface, even at the inner part of the film. However, misaligned plate-like crystals were also found, and these crystals were thought to suppress the formation of the highly grain-aligned microstructure at the inner region. These disordered grain regions might be formed during the first sintering and the intermediate pressing did not improve the grain orientation because randomly oriented Bi2223 crystals generally formed in the samples during the first sintering, except for the region near the Ag surfaces. The mean misalignment angle of the crystals, which was calculated by averaging the misalignment angle of 93 crystals existing in the lower left quarter part of this picture, was ~15°. It was reported that the mean misalignment angle of the crystals in the practical Bi2223 tapes with a high I_c of ~200 A at 77 K was ~6° and the I_c of the tapes decreased logarithmically with an increase in the mean misalignment angle [19]. Therefore, this disorder of orientation might significantly suppress the J_c properties of the film samples. This image also reveals that the relative density of this film was ~90%, meaning that the dense Bi2223 polycrystalline samples were successfully prepared in this study. In contrast, the grain size at the inner part of the

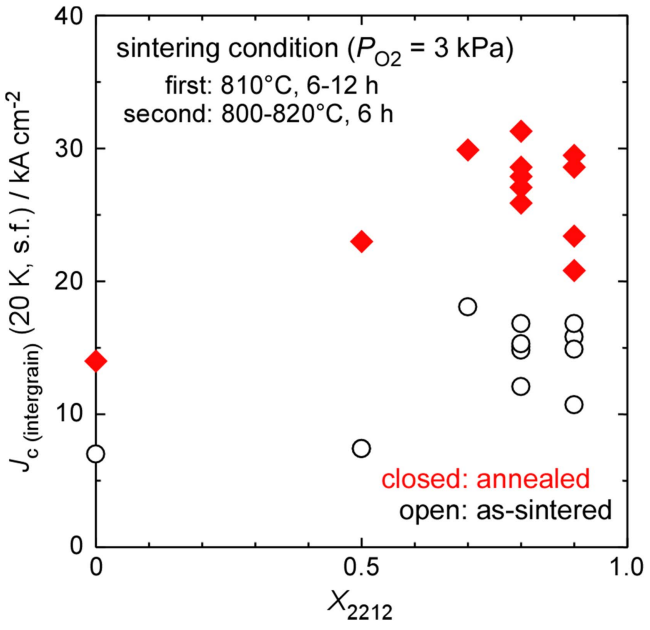

Figure 4. Relationship between X_{2212} and $J_{c\ (intergrain)}$ at 20 K in the self-field of the various film samples.

Table 1. Nominal Pb substitution composition (x (nominal)), the c-axis length and Pb substitution composition analyzed by WDS (x (analyzed)) of the typical $Bi_{2-x}Pb_xSr_2Ca_2Cu_3O_y$ film samples after the second sintering under $P_{O2} = 3$ kPa. The c-axes lengths were evaluated after controlling the oxygen content of the samples by annealing in air at 600 °C and quenching to room temperature.

x (nominal)	c-axis length [Å]	x (analyzed)
0.35	37.144(1)	0.339(5)
0.37	37.139(1)	0.357(5)
0.39	37.130(1)	0.385(3)

film was found to be less than 5 μm, which is much smaller than that near the surface, >10 μm, as shown in figure 2(b). This suggests that the grain growth during the sintering process was not sufficient to achieve a high J_c in the region away from the interface with Ag foil.

The effects of the microstructure control described above on the grain coupling characteristics were examined. The relationship between X_{2212} and $J_{c\ (intergrain)}$ at 20 K in the self-field of the various film samples is summarized in figure 4. The samples after the second sintering are expressed as 'as-sintered', and 'annealed' plots indicate the samples post-annealed in a reducing atmosphere (at 760 °C for 48 h under $P_{O2} = 500$ Pa) and finally oxygen annealed (at 350 °C for 6 h). Surface XRD studies revealed that the Pb3221 phase did not generate during these annealing processes. The $J_{c\ (intergrain)}$ of the films was enhanced with larger X_{2212}, corresponding to their strongly c-axis-oriented surface microstructure. The 'annealed' samples showed a higher $J_{c\ (intergrain)}$ than the 'as-sintered' samples with the same X_{2212} value, which suggests that controlling the chemical compositions by annealing after the second sintering was effective in improving $J_{c\ (intergrain)}$. The highest $J_{c\ (intergrain)}$ of 32 kA cm^{-2} at 20 K was achieved in a sample with $X_{2212} = 0.8$, sintered at 810 °C for 12 h (the first sintering) and 6 h (the second sintering). In contrast, the c-axis orientation in the surface of the sample with $X_{2212} = 0.9$ estimated by XRD was better than that of the sample with $X_{2212} = 0.8$. Since our previous study on the Bi2223 sintered bulks indicated that a strong grain connection among fine grains was easily formed during the second sintering process [12], the existence of relatively large Bi2223 grains in the samples with $X_{2212} = 0.9$ after the first sintering might suppress $J_{c\ (intergrain)}$ properties.

In this section, it was revealed that a high $J_{c\ (intergrain)}$ was achieved in the thick film samples with $X_{2212} = 0.8$ by forming a dense and c-axis grain-oriented microstructure. The annealing processes controlling the nonstoichiometric chemical compositions were also confirmed to be effective in improving the grain coupling.

3.2. Improvement of intergrain J_c properties by increasing the Pb-doping level

Since the Bi2223 thick films with $X_{2212} = 0.8$ showed a relatively high $J_{c\ (intergrain)}$ by controlling the microstructure as described above, this strategy was applied to prepare thick films with various Pb substitution levels. It has been suggested that it is difficult to form heavily Pb-doped Bi2223 phases [20], which means that film samples with degraded microstructures might be obtained by increasing the Pb substitution level, x. Recently, we have successfully synthesized Pb-rich Bi2223 sintered bulks with relatively larger x by sintering calcined powders with $x = 0.45$ and 0.55 at 800 °C under $P_{O2} = 1$ kPa [21]. By employing 2223 powder with $x \sim 0.45$ or 0.55 prepared by pulverizing these Pb-rich Bi2223 sintered bulks and 2212 powder with $x = 0.35$, the nominal x of the film samples with $X_{2212} = 0.8$ was varied from 0.35 to 0.37 or 0.39. In addition, the formation reaction of the Bi2223 phase occurs only from 2212 powder with $x = 0.35$ in this method, meaning that this reaction should finish and the c-axis-oriented microstructure will be formed, even in the relatively short first sintering, as demonstrated above. According to this idea, the thick film samples with $x \sim 0.35$, 0.37 and 0.39 were prepared by sintering at 810 °C under $P_{O2} = 3$ kPa.

The surface XRD of the samples first sintered for 12 h suggested that Bi2223 was the main phase, and the 00 l peaks of the Bi2223 phase with a relatively strong intensity originating in the c-axis-oriented grains were observed in all samples, regardless of the Pb substitution level, x. Moreover, the surface XRD and secondary electron images suggested that c-axis orientation near the surface of each sample was further strengthened after the second sintering for 6 h. As in the case of $x = 0.35$ shown in figure 2(b), the typical grain size of the second-sintered thick film samples with various x was >10 μm, and these samples maintained a similarly strong c-axis orientation at their surfaces. The nominal Pb composition (x (nominal)), the c-axis length and Pb composition analyzed by WDS (x (analyzed)) for the typical film samples after the second sintering are shown in table 1. The c-axes lengths and x (analyzed) values were systematically changed with an increase in x (nominal). This strongly suggests that

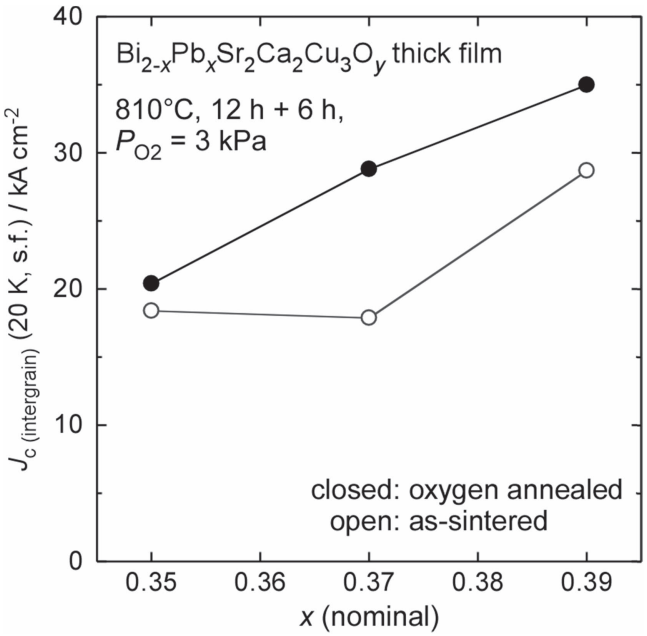

Figure 5. $J_{c\ (intergrain)}$ at 20 K of the film samples with various x (nominal) before and after oxygen annealing at 300 °C.

samples with a higher actual Pb substitution level were successfully prepared. The standard deviation of x (analyzed) of ~10% was not large, even in the samples with $x = 0.37$ and 0.39, which suggests that a diffusion of lead ions from the Pb-rich Bi2223 crystals quickly occurred during the sintering, and films with relatively homogeneous Pb substitution levels were obtained. On the other hand, T_c (onset) evaluated by magnetic susceptibility measurements under 10 Oe of these film samples after oxygen annealing at 300 °C was ~108 K, regardless of x. Enhancement of the hole carrier concentration by the progress of Pb doping was not verified from the change in T_c.

However, the effects of the slight increase in x on the superconducting properties of the polycrystalline films clearly appeared in the J_c properties. Figure 5 shows the $J_{c\ (intergrain)}$ at 20 K of these samples after the second sintering (as-sintered), and additional oxygen annealing at 300 °C for 12 h (oxygen annealed). Note that reductive post annealing to control the nonstoichiometric cation compositions was not performed for these samples. The $J_{c\ (intergrain)}$ of the samples tended to be enhanced with an increase in the Pb-doping level. This suggests that the carrier slightly overdoped state and the lower anisotropy of Bi2223 by Pb substitution, as in the case of Pb-rich Bi2212 [14, 15], contributed to the improvement of $J_{c\ (intergrain)}$. In addition, this enhancement in $J_{c\ (intergrain)}$ was noticeable in the oxygen annealed samples because the increase in carrier concentration and reduction of the anisotropy of Bi2223 progressed further by raising the excess oxygen content. Therefore, it was found that the slight increase in the Pb substitution level, as well as appropriate oxygen annealing, were effective in improving the $J_{c\ (intergrain)}$ of Bi2223 polycrystalline materials by additional carrier doping and lowering the anisotropy.

Controlling the nonstoichiometric cation compositions of the films with $x \sim 0.39$, which exhibited a relatively high $J_{c\ (intergrain)}$ even after the second sintering, was attempted by reductive post annealing. In the samples with $x \sim 0.35$, post annealing to control the cation compositions close to the integral ratio was performed at 760 °C for 48 h under $P_{O2} = 500$ Pa. Enhancement in the T_c by ~2 K and an extension of the c-axis were observed in the samples after reductive post annealing. However, the T_c of the samples with $x \sim 0.39$ did not change before and after post annealing under this condition, which suggests that the reaction to control the nonstoichiometric cation compositions did not progress through annealing. Then, the reductive post annealing conditions for the samples with $x \sim 0.39$ were optimized. Post annealing for a long period of time under $P_{O2} = 500$ Pa was found to be effective in enhancing T_c and extending the c-axis in accordance with the control of the cation compositions, though such a long post annealing might accompany the generation of Pb3221 precipitates. On the other hand, it was also confirmed that the Pb3221 precipitates in the samples disappeared after additional post annealing under lower oxygen pressure, $P_{O2} = 200$ Pa, because of the re-progress of the solid solution reaction of divalent lead ions. Therefore, we determined the optimal reductive post-annealing condition, which was annealing at 760 °C for 100 h under $P_{O2} = 500$ Pa, and additionally at 760 °C for 48 h under $P_{O2} = 200$ Pa. A slightly Pb-rich film sample ($x \sim 0.39$) with controlled nonstoichiometric cation compositions and without Pb3221 precipitates was successfully obtained by post annealing under this condition.

Improvement in the superconducting properties of the samples by controlling the cation compositions is discussed. Temperature dependences of the irreversibility field and $J_{c\ (intergrain)}$ in the self-field for the film samples finally oxygen annealed at 300 °C are shown in figures 6 and 7, respectively. The sintering conditions of these samples were the same as the samples demonstrated in figure 5 (810 °C, 12 h + 6 h, $P_{O2} = 3$ kPa). The irreversibility field and $J_{c\ (intergrain)}$ of the annealed samples, which were post annealed in a reducing atmosphere under each optimal condition and thought to have controlled cation compositions, were higher than that of the as-sintered samples when we compare them with the same x. In particular, the irreversibility field of the annealed samples was found to be almost two times higher by controlling the cation compositions. Moreover, the high Pb-doping level was confirmed to be effective in improving the superconducting properties. Increasing the hole carrier concentration and lowering the anisotropy of Bi2223 by the progress of Pb substitution were effective in improving the J_c properties in the magnetic fields as well. A combination of controlling the nonstoichiometric cation compositions by reductive post annealing and increasing the Pb substitution level was confirmed to be a promising way to improve the grain coupling of the Bi2223 polycrystalline materials. The irreversibility field and $J_{c\ (intergrain)}$ were enhanced by almost three and two times, respectively, through this combination method. The highest $J_{c\ (intergrain)}$ values of ~50 kA cm^{-2} and ~8 kA cm^{-2} in the self-field at 4.2 K and 77 K, respectively, were recorded by

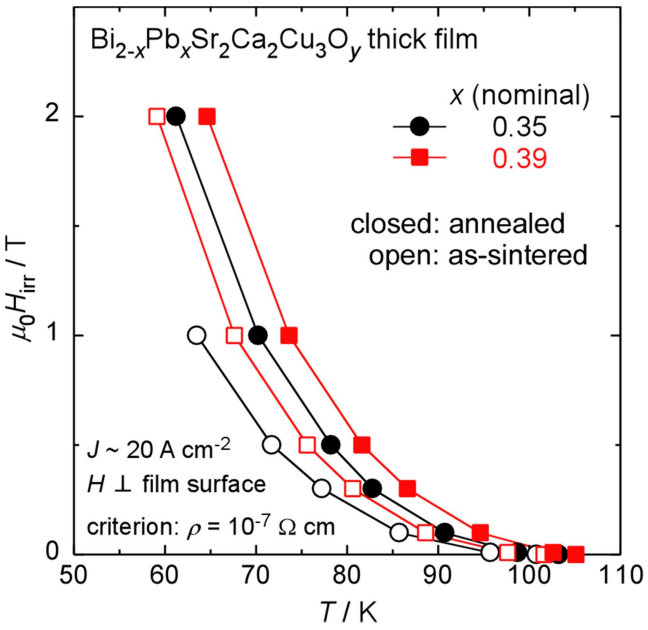

Figure 6. Temperature dependence of the irreversibility field for the oxygen-annealed film samples.

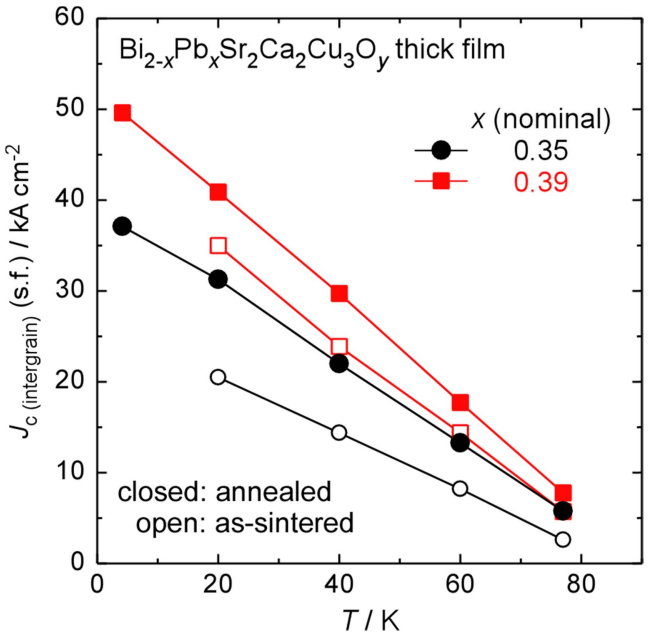

Figure 7. Temperature dependence of $J_{c\ (intergrain)}$ for the oxygen-annealed film samples.

the Pb-rich sample post-annealed under a reducing atmosphere. However, the amount of improvement in $J_{c\ (intergrain)}$ by reductive post annealing of the sample with $x \sim 0.39$ was smaller than that of the sample with $x \sim 0.35$. This means that controlling the cation compositions was still not enough to achieve a high $J_{c\ (intergrain)}$ in the sample with $x \sim 0.39$. The $J_{c\ (intergrain)}$ of the samples with Pb-rich compositions could be further improved by a more precise control of the cation compositions close to the integral ratio.

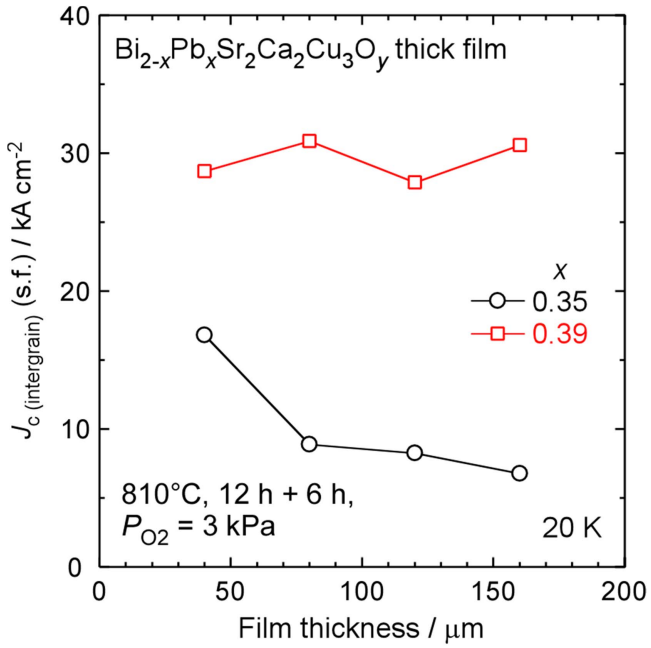

Figure 8. Film thickness dependence of $J_{c\ (intergrain)}$ of the film samples with $x = 0.35$ and 0.39.

3.3. Fabrication of high I_c films by increasing the film thickness

The J_c properties of Bi2223 thick films are found to be improved by controlling the microstructure and chemical compositions. However, thick film materials with high I_c properties are needed for various applications. The fabrication of high I_c films was attempted by increasing the film thickness from ~40 μm. The thickness of the film was controlled by the number of stacking green films on Ag foil substrates.

In order to examine the dependence of the critical current properties on the film thickness, the samples with $x = 0.35$ and 0.39 were prepared under the same sintering condition (810 °C, 12 h + 6 h, $P_{O2} = 3$ kPa) as the 'as-sintered' samples described in figure 5. The thicknesses of the resulting samples were controlled to be ~40, ~80, ~120 and ~160 μm. Surface XRD suggested that all the samples were composed almost entirely of the Bi2223 phase and had *c*-axis-oriented surfaces after the second sintering. SEM observation of the fractured surfaces of the samples with various thicknesses revealed that the actual film thicknesses almost agreed with their nominal thicknesses. The film thickness dependence of $J_{c\ (intergrain)}$ of the film samples at 20 K is shown in figure 8. It should be noted that these samples were not annealed to control the nonstoichiometric chemical compositions. The $J_{c\ (intergrain)}$ of the samples with $x = 0.35$ decreased with an increase in the film thickness, and hence I_c values were thought to be slightly enhanced in the thicker films. As shown in figure 3, many misaligned Bi2223 grains exist at the inner part of the film. In the thicker films, the volume fraction of the poor grain-aligned region increases, resulting in suppressed J_c properties. On the other hand, the samples with $x = 0.39$ exhibited relatively high $J_{c\ (intergrain)}$, even in the thicker films, which means high I_c properties

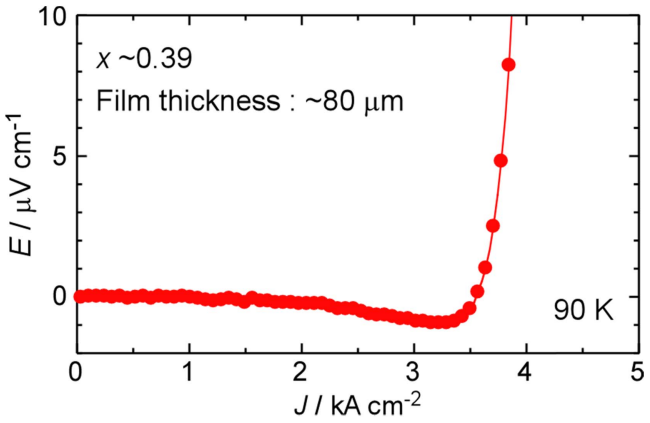

Figure 9. *E–J* curve at 90 K of a Bi2223 thick film with $x = 0.39$ and $\sim 80\ \mu m^t$.

could be achieved with a larger film thickness. This suggests that the J_c of the *c*-axis direction was enhanced by lowering the anisotropy of Bi2223 with the Pb-rich composition, which enabled a larger current to flow in the whole of the thicker films. This relatively high J_c of the thicker film was also confirmed by evaluating the transport properties of the film with $\sim 80\ \mu m^t$ at 90 K in the self-field, as shown in figure 9. A small declination of the *E–J* curve around $J = 3\ kA\ cm^{-2}$ in figure 9 is not considered as intrinsic behavior, which might be due to the non-uniform temperature distribution around the sample holder. High transport J_c was achieved in this film, meaning that this film could carry larger I_c owing to the larger effective current path by increasing the film thickness.

The I_c properties were found to be enhanced with an increase in the film thickness in the Pb-rich film samples. A high I_c of $>10^2$ A at high temperatures such as 77 K should be exhibited in thicker films with controlled nonstoichiometric chemical compositions by the reductive and oxygen annealing demonstrated above. Such a high I_c is a promising attribute suitable for various applications, such as current leads and magnetic shields.

4. Conclusion

We have attempted to develop Bi2223 thick film materials with high critical current properties by controlling their microstructures and applying chemical approaches. It was revealed that employing precursor powder composed of most of the unreacted phases and containing Bi2223 grains by ~20% was effective in forming the Bi2223 phase rapidly and a *c*-axis-oriented microstructure. Reductive post annealing and oxygen annealing processes to control the nonstoichiometric chemical compositions were confirmed to enhance $J_{c\ (intergrain)}$. Moreover, an increase in the actual Pb substitution level for the Bi site in Bi2223 was found to improve the critical current properties both in the self-field and under magnetic fields by enhancing the hole carrier concentration and decreasing the anisotropy. The highest J_c values of $\sim 50\ kA\ cm^{-2}$ and $\sim 8\ kA\ cm^{-2}$ in the self-field at 4.2 K and 77 K, respectively, were achieved in the thick film sample with $\sim 40\ \mu m^t$. These $J_{c\ (intergrain)}$ values of the thick film are almost four times higher than that of the sintered bulk in our previous study [12]. Largely improved J_c properties in the thick film were achieved by forming a dense and partly *c*-axis-oriented microstructure and by increasing the Pb substitution level. On the other hand, thicker films with a Pb-rich composition could exhibit a higher I_c, which suggests that thick films are promising materials for use in various current-carrying applications.

However, there is room for improvement in the $J_{c\ (intergrain)}$ of the thick films in terms of the microstructure and the chemical composition. Enhancement of the degree of the *c*-axis orientation of grains, including the inner part of the films, is crucially important for the former, which might logarithmically enhance $J_{c\ (intergrain)}$. Further research into high-quality chemical approaches, such as more precise control of the cation compositions close to the integral ratio and optimizations of the Pb-doping level and the oxygen content, is needed for the latter. These refinements in the fabrication conditions of polycrystalline materials should enable us to synthesize Bi2223 thick films or sintered bulks with a high J_c of $> 10^4\ A\ cm^{-2}$ at 77 K comparable to the engineering J_c of practical Ag-sheathed tapes.

ORCID iDs

Y Takeda https://orcid.org/0000-0001-7217-9853
T Motoki https://orcid.org/0000-0003-3218-0977

References

[1] Nakashima T, Kobayashi S, Kagiyama T, Yamazaki K, Kikuchi M, Yamade S, Hayashi K, Sato K, Osabe G and Fujikami J 2012 *Cryogenics* **52** 713–8
[2] Yumura H *et al* 2013 *IEEE Trans. Appl. Supercond.* **23** 5402306
[3] Sato K, Kobayashi S and Nakashima T 2012 *Japan. J. Appl. Phys.* **51** 010006
[4] Hashi K *et al* 2015 *J. Magn. Reson.* **256** 30–3
[5] Ishizuka M and Sakuraba J 2006 *Physica* C **433** 173–81
[6] Asano T, Tanaka Y, Fukutomi M, Jikihara K, Machida J and Maeda H 1988 *Japan. J. Appl. Phys.* **27** L1652–4
[7] Kobayashi S *et al* 2005 *IEEE Trans. Appl. Supercond.* **15** 2534–7
[8] Shimoyama J, Kato T, Kobayashi S, Yamazaki K, Hayashi K and Sato K 2005 *Japan. J. Appl. Phys.* **44** L1525–8
[9] Dou S X, Liu H K, Zhang Y L and Bian W M 1991 *Supercond. Sci. Technol.* **4** 203–6
[10] Yuan Y, Cai X Y, Jiang J, Huang Y, Larbalestier D C and Hellstrom E E 2005 *IEEE Trans. Appl. Supercond.* **15** 2530–3
[11] Watanabe M, Shimoyama J, Obata K, Kishio K, Kobayashi S and Hayashi K 2011 *IEEE Trans. Appl. Supercond.* **21** 2812–5
[12] Takeda Y, Shimoyama J, Motoki T, Kishio K, Nakashima T, Kagiyama T, Kobayashi S and Hayashi K 2017 *Physica* C **534** 9–12

[13] Maeda A, Hase M, Tsukada I, Noda K, Takebayashi S and Uchinokura K 1990 *Phys. Rev.* B **41** 6418–34
[14] Motohashi T, Nakayama Y, Fujita T, Kitazawa K, Shimoyama J and Kishio K 1999 *Phys. Rev.* B **59** 14080–6
[15] Régi F X, Schneck J, Savary H, Mellet R and Daguet C 1993 *Appl. Supercond.* **1** 627–34
[16] Ueda S, Shimoyama J, Horii S and Kishio K 2007 *Physica* C **452** 35–42
[17] Tajima R, Shimoyama J, Yamamoto A, Ogino H, Kishio K, Nakashima T, Kobayashi S and Hayashi K 2013 *IEEE Trans. Appl. Supercond.* **23** 6400604
[18] Zhang L, Mironova M, Selvamanickam V and Salama K 2000 *Physica* C **341-348** 1471–2
[19] Ayai N *et al* 2007 *IEEE Trans. Appl. Supercond.* **17** 3075–8
[20] Majewski P 1997 *Supercond. Sci. Technol.* **10** 453–67
[21] Takeda Y *et al* 2017 *Abstr. CSSJ Conf.* **94** 186 (in Japanese)